Science of the Total Environment 505 (2015) 367–375

Contents lists available at ScienceDirect

Science of the Total Environment

journal homepage: www.elsevier.com/locate/scitotenv

A new look at inhalable metalliferous airborne particles on rail subway platforms

Teresa Moreno [a,*], Vânia Martins [a,b], Xavier Querol [a], Tim Jones [c], Kelly BéruBé [d], Maria Cruz Minguillón [a], Fulvio Amato [a], Marta Capdevila [e], Eladio de Miguel [e], Sonia Centelles [e], Wes Gibbons [f]

[a] Institute of Environmental Assessment and Water Research (IDÆA-CSIC), C/Jordi Girona 18-24, 08034 Barcelona, Spain
[b] Dept. of Analytical Chemistry, Faculty of Chemistry, University of Barcelona, Av. Diagonal 647, 08028 Barcelona, Spain
[c] School of Earth and Ocean Sciences, Cardiff University, CF10 3YE Cardiff, Wales, UK
[d] School of Biosciences, Cardiff University, Museum Avenue, Cardiff CF10 3AX, Wales, UK
[e] Transports Metropolitans de Barcelona (TMB), Santa Eulalia 08902, Av. del Metro s/n L'Hospitalet de Llobregat, Spain
[f] WPS, C/Major 13, 08870 Sitges, Spain

HIGHLIGHTS

- Most particles breathed on subway platforms are ferruginous and nanometric in size.
- Particles derive dominantly from mechanical processes at brake–wheel–rail interface.
- Fe-particles have a flake shape with inhomogeneous chemistry (Ba/Zn/Cu).
- Fe-PM undergoes progressive atmospheric oxidation from metal Fe to magnetite/hematite.
- It is still unclear whether subway air is more or less toxic than outdoor air.

ARTICLE INFO

Article history:
Received 5 August 2014
Received in revised form 2 October 2014
Accepted 4 October 2014
Available online 18 October 2014

Editor: P. Kassomenos

Keywords:
Subway PM
Platform air quality
SEM
TEM
Iron oxides
Nanoparticles

ABSTRACT

Most particles breathed on rail subway platforms are highly ferruginous (FePM) and extremely small (nanometric to a few microns in size). High magnification observations of particle texture and chemistry on airborne PM_{10} samples collected from the Barcelona Metro, combined with published experimental work on particle generation by frictional sliding, allow us to propose a general model to explain the origin of most subway FePM. Particle generation occurs by mechanical wear at the brake–wheel and wheel–rail interfaces, where magnetic metallic flakes and splinters are released and undergo progressive atmospheric oxidation from metallic iron to magnetite and maghemite. Flakes of magnetite typically comprise mottled mosaics of octahedral nanocrystals (10–20 nm) that become pseudomorphed by maghemite. Continued oxidation results in extensive alteration of the magnetic nanostructure to more rounded aggregates of non-magnetic hematite nanocrystals, with magnetic precursors (including iron metal) still preserved in some particle cores. Particles derived from steel wheel and rails contain a characteristic trace element chemistry, typically with Mn/Fe = 0.01. Flakes released from brakes are chemically very distinctive, depending on the pad composition, being always carbonaceous, commonly barium-rich, and texturally inhomogeneous, with trace elements present in nanominerals incorporated within the crystalline structure. In the studied subway lines of Barcelona at least there appears to be only a minimal aerosol contribution from high temperature processes such as sparking. To date there is no strong evidence that these chemically and texturally complex inhalable metallic materials are any more or less toxic than street-level urban particles, and as with outdoor air, the priority in subway air quality should be to reduce high mass concentrations of aerosol present in some stations.

1. Introduction

With nearly 200 rail subway systems in operation worldwide, transporting more than 100 million people daily, air quality both on station platforms and inside trains is an important urban air pollution issue (Nieuwenhuijsen et al., 2007). Average return journey times last around

* Corresponding author. Tel.: +34 934006123.
E-mail address: teresa.moreno@idaea.csic.es (T. Moreno).

http://dx.doi.org/10.1016/j.scitotenv.2014.10.013

one hour so that many underground rail commuters are routinely exposed to transient doses of inhalable particulate matter (PM) levels higher than the 50 μg/m^3 mean PM_{10} (PM <10 μm in size) limit legally imposed for outdoor European city air. In fact, PM levels are commonly much higher than those above ground, as demonstrated by an array of recently published studies in subway systems from cities as varied as Los Angeles, Barcelona, Milan, Paris, Prague, Rome, Stockholm, Seoul, Shanghai and Taipei (Fromme et al., 1998; Johansson and Johansson, 2003; Seaton et al., 2005; Braniš, 2006; Ripanucci et al., 2006; Salma et al., 2007; Kim et al., 2008; Park and Ha, 2008; Raut et al., 2009; Ye et al., 2010; Cheng and Yan, 2011; Kam et al., 2011; Querol et al., 2012; Colombi et al., 2013; Moreno et al., 2014). More interesting than the simple elemental mass concentration of inhalable PM is the fact that these particles have a peculiar physico-chemical character specific to the subway environment, being loaded with inhalable ferruginous particles (FePM) commonly accompanied by other elements such as C, Si, Ca, Mn, Cr and Ba.

It has been argued that the metalliferous character of the particles produced by underground rail transport has a considerable potential capacity to stimulate reactive oxygen species (ROS) generation and cause DNA damage (M. Jung et al., 2012), especially since the work of Karlsson et al. (2005), who presented toxicological evidence apparently in favour of enhanced genotoxicity for subway PM. Not only is the particle chemistry implicated in this concept of enhanced toxicity, but also the range of sizes, morphologies and surface bioreactivities are likely to differ from those more typical of outdoor urban PM (Knibbs et al., 2011). Of key interest here is FePM morphology and the speciation of the inhalable ferruginous material, as some iron species are reported to be more toxic than others (Park et al., 2014).

Our understanding of the origin and potential toxicity of subway particles is limited by the fact that there have been relatively few studies elucidating the detailed morphology and chemistry of individual inhalable aerosols. Indeed, reviewing the available literature there is still uncertainty over some issues, such as the exact speciation of ferruginous particles available for inhalation on station platforms, the importance of mechanical versus thermal processes in subway particle generation, and the relative importance and origins of other elements also present in FePM. In the context of subway particle physicochemical characterisation there is in particular a striking lack of high quality imaging of subway PM at high magnification. Several papers have published secondary electron images, but these usually provide only limited information about the range of particle types that exist in the samples and are not the main focus of the study (e.g. Abbasi et al., 2012, 2013; HJ. Jung et al., 2012; Loxham et al., 2013; Midander et al., 2012; Múgica-Alvarez et al., 2012; Murruni et al., 2009).

This paper aims to contribute to and clarify the debate about the character of subway air by presenting and interpreting high magnification images and chemical analyses obtained during an ongoing study conducted on samples collected from the Barcelona Metro. This subway system, operated by Transports Metropolitans de Barcelona (TMB), carries a large proportion of the city daily commute, around 1.25 million people (Moreno et al., 2014). Here we focus in particular on the ferruginous particles that dominate subway platform air, and on the significant contribution from inhalable-sized carbonaceous polymetallic particles interpreted to be derived from the application of asbestos-free pneumatic brakes.

2. Methodology

The subway aerosol PM examined for this study was collected during an intensive monitoring campaign carried out over four months (April–July 2013) at different stations within the Barcelona Metro system. Barcelona's Metro includes 11 metro lines built since 1929 to 2010, the latest (L9–L11) with platform screen door systems and advanced ventilation systems. All trains are operated electrically (80% of them being motor carriages) and run from 5 a.m. until midnight every day, with additional services on Friday nights (finishing at 2 a.m. of Saturday) and Saturday nights (running all night long), with a frequency between 2 and 15 min, depending on the day (weekend or weekday) and time of day. Night maintenance works involving diesel vehicles or yielding operations are occasional but can have an impact on the platform air quality.

The braking system is electric when approaching the platform, changing to non-asbestos pneumatic braking when slowing down below a 5 km/h velocity for all lines independently of the platform design, using either frontal or lateral brake pads.

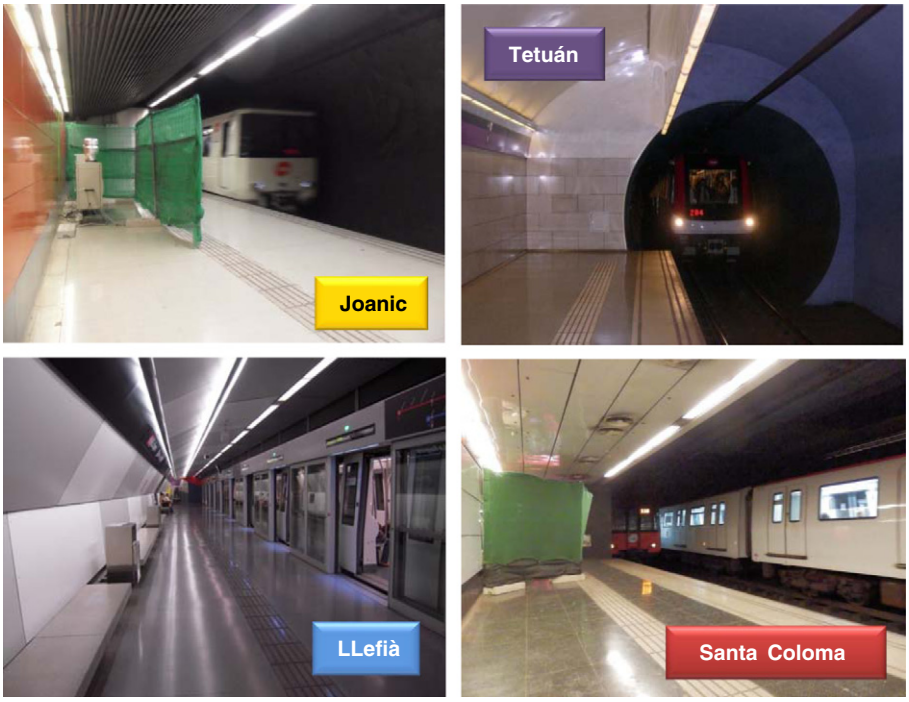

Fig. 1. Stations selected for the study. Santa Coloma (Line 1), Tetuan (Line 2), Joanic (Line 4), and Llefià (in the new sliding door system Line 10).

At all sampling sites subway platform PM_{10} was collected on polyurethane foam substrates (PUF) during 8 consecutive days (from 9:00 a.m. on Monday to 9:00 a.m. of Tuesday of the following week) using an Airborne Sample Analysis Platform system (ASAP; Model 2800 Thermo, USA) with a high sample flow-rate of 200 l/min. The equipment was located at the end of the platform corresponding to the entrance point of the train into the station, with no exit access to minimise the complexity of air turbulence and annoyance to passengers. Four stations were selected (Fig. 1), each with different designs chosen to obtain a wide range of PM sample characteristics, including a station with open double rail track (Santa Coloma), double track separated by a wall in the station (Joanic), single rail track (Tetuan) and a new station with platform screen doors (PSD's) separating the single rail track from the platform (Llefià).

Individual particles were characterised using scanning electron microscopy. The size and shape of individual particles were observed using a JEOL5900LV Scanning Electron Microscope (SEM) via an energy dispersive X-ray microanalysis system (EDX). PUF substrates were directly 'flat-mounted' onto aluminium SEM stubs using epoxy-resin (Araldite) as an adherent between the PUF and the stub. The samples were then gold/palladium-coated using a 208HR Sputter Coater (Cressington, UK) and an MTM20 Thickness Controller (Cressington, UK). The microscope working distance was 10 mm, with an accelerating voltage of 20 kV.

In addition, sampled particles were visualised using a high resolution transmission electron microscope (HR-TEM). For this, particles were suspended in molecular biology (MB) grade water (Sigma-Aldrich, UK; 2 μg PM/1 μl H_2O) and 40 μl of this suspension was pipetted onto the surface of a 200 mesh Au grid with carbon film (Agar Scientific). Samples were imaged using a Philips CM12HR-TEM at 80 kV accelerating voltage, and images were obtained with a SIS MegaView III digital camera.

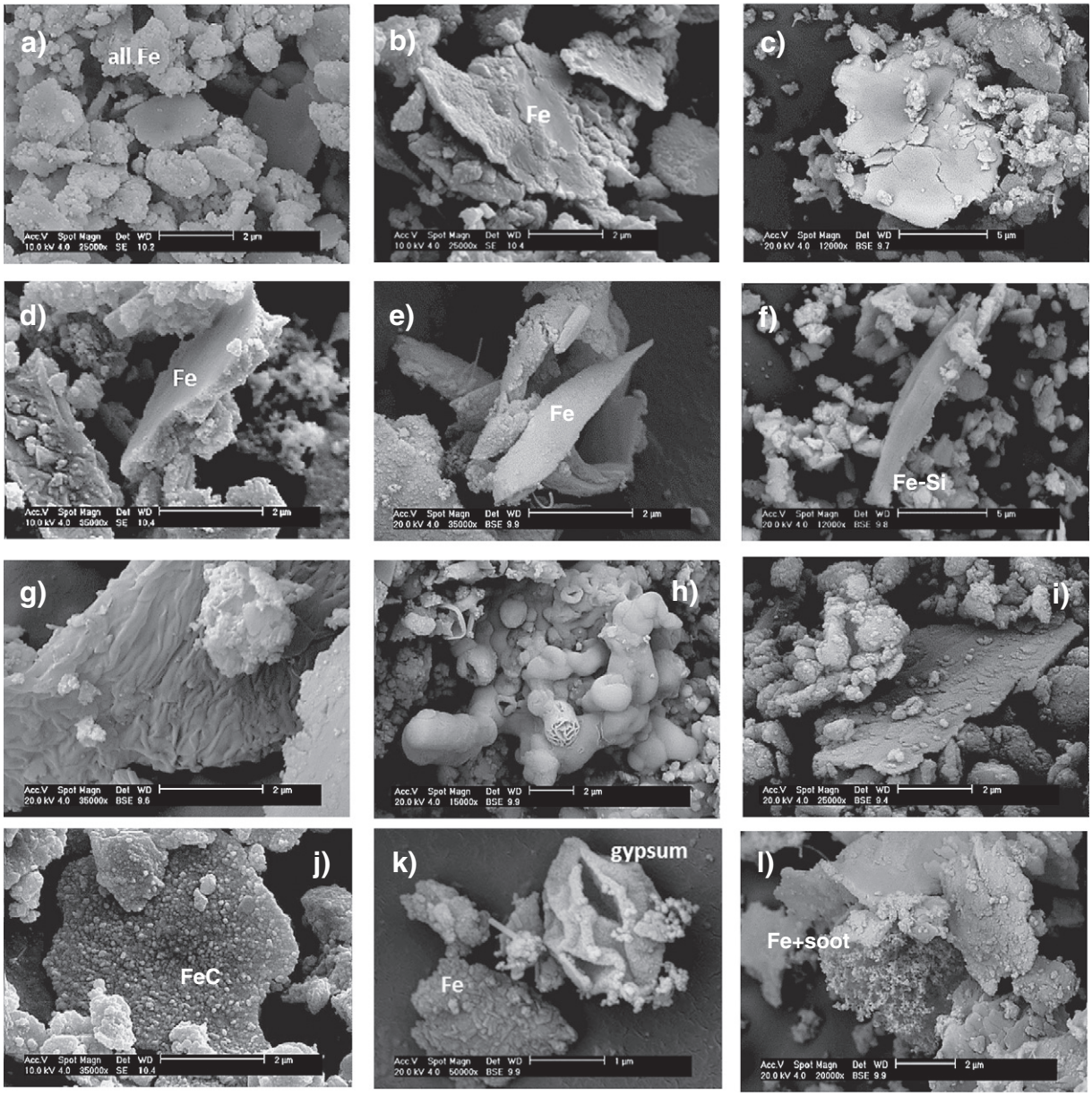

Fig. 2. SEM images demonstrating the typical morphological aspect of FePM in subway samples: a) General aspect of a PUF sample with subway PM_{10} dominantly ferruginous and flake-like; b–f) FePM with flake and splintery morphologies; g) Lineated FePM flake; h) Botryoidal morphology interpreted as hematite; i) Large FePM flake with rough, coarsely cleaved surface and attached nanoparticles; j) FeCPM with nanometric crystals growing on the flake surface; k) FePM flake adjacent to amorphous gypsum (calcium sulphate) particle on which has grown nanometric crystalline needles of new gypsum; l) FePM flakes and carbonaceous nanometric soot aggregates.

3. Results

Particle concentrations (8 day means) were highest in the double rail track station (Santa Coloma 72 μg $PM_{2.5}/m^3$), followed by the station with single rail track (Tetuan 44 μg $PM_{2.5}/m^3$), whereas the stations with a wall separating both rail tracks (Joanic) and the sliding door system (Llefià) both had values of 29 μg $PM_{2.5}/m^3$. These variations in PM mass concentration were mostly related to the differences in platform design and ventilation rather than particle sources, because particle composition and morphologies were very similar in all stations (as observed after studying the samples under SEM), indicating a common mechanism of formation. Compositionally the most abundant particles were Fe-rich (Fig. 2a), in agreement with the previous subway studies elsewhere (e.g. Aarnio et al., 2005; Kang et al., 2008; Salma, 2009; HJ. Jung et al., 2012; Midander et al., 2012; Minguillón et al., 2012). Indeed, it is difficult to analyse a subway particle that does not register at least some iron, an observation that we shall discuss further below.

The inhalable-sized fraction of ferruginous particles (FePM) in the Barcelona subway samples displays a spectrum of morphologies under the SEM, but by far the most common occurs in the form of irregular, rough-surfaced flakes measuring at most just a few microns in size (Fig. 2a), with the larger examples commonly displaying cracked and corroded textures (Fig. 2b, c). Sharply angular shard-like and splintery forms often with relatively smooth surfaces (Fig. 2d, e, f) are also common in the FePM, and a range of other textures include lineated (Fig. 2g), botryoidal (Fig. 2h), or roughly cleaved (Fig. 2i). It is normal to observe nanometric PM attached to the host particle (Fig. 2c, i, j, l), indeed, in terms of particle number, submicron FePM is the most abundant type.

Many FePM flakes are carbonaceous, with C being present either integrated within the grain structure or as nanometric crystals growing on the surface (Fig. 2j). In addition, more familiar carbonaceous particles within the subway PM_{10} samples include diesel soot attached to the host FePM (Fig. 2l), and biological aerosols (Fig. 3a, b, c, d) introduced probably from outside city air. Coarser PM_{10} (>5 μm) is much rarer in these samples, and is more commonly associated with "geological" particles such as quartz, calcium carbonate, calcium sulphates (from soil and building materials) and both aluminium and iron–magnesium silicates. Halite particles are also present, commonly in the shape of euhedral cubic crystals that have grown within the PUF substrate after sample collection (Fig. 3e). Metals other than Fe, although detected at trace levels in the chemical analyses of PM filter bulk samples, are only rarely evident under the SEM. Barium sulphates were observed in both old and new stations (Santa Coloma and Llefià), these being attributed to the use of barite in the fabrication of brakes in both trains and road vehicles (Aarnio et al., 2005). Other trace metals identified under the SEM include Zn, Ti, and Sb, the latter again most probably related to brake abrasion and always attached to or integrated within larger particles (Fig. 3f–i). Occasional bright spots under SEM backscatter reveal concentrations of Sb, either in irregular, sub-angular grains associated with Ca (also present in brakes as calcite), or as spheres with associated traces of S and V. Copper PM was only identified in the samples from Joanic and Santa Coloma, the two stations where the pantograph connecting to the electric supply catenary (which is made of 95% Cu wire) is made of copper or graphite (50% of trains each), whereas it is only graphite in the other two stations. These trace metallic particles in the subway samples are always in the nanosized scale and occur either embedded obscurely within ferruginous masses or adhered to the surface of larger particles, with morphologies ranging from amorphous to spherical. In general micrometric metallic spheres are not common in the Barcelona Metro samples which are overwhelmingly dominated by ferruginous flakes and splinters.

In order to elucidate further the chemistry of subway platform FePM at high magnifications, Table 1 provides a selection of analyses of micrometric sized areas viewed under the transmission electron microscope (similar to the data shown in the chemical maps of Fig. 4) comparing PM from new and old lines. All areas analysed in this way were highly ferruginous (Fe 40–65 wt.%), and when Mn was registered as an accompanying minor element this was almost always in the ratio of Mn/Fe = 0.01. In addition, the TEM analyses confirm the carbonaceous character of many FePM, and our data suggest the presence of at least three groups based on carbon contents registered as low C (<5 wt.%), medium C (10–20 wt.%) or high C (>40 wt.%) (Table 1). Both Si and Ca are commonly present, as are traces of other elements Al, Mg, Na, K, Cr, Co, Sb, S, and Cl (Table 1). These analyses provide some clear indicators as to the likely source materials responsible for subway FePM generation. A Mn/Fe ratio of 0.01 is highly consistent with an origin from steel used in wheels, rails and brakes (Abbasi

Table 1
Chemical composition (elemental weight %) obtained by TEM microanalysis from typical FePM images of the Barcelona subway samples comparing particles from the new and old lines. See text for discussion. Cu was not analysed as it is the major component of the sample holder in the TEM.

Element (wt.%)	New line				Old line				
C	1.96	3.46	12.35	12.83	18.46	19.52	13.72	49.85	11.06
O	22.23	32.47	9.08	22.01	18.65	16.42	21.01	4.73	15.12
Na	0.86	1.87	0.62	0.25	0.89	0.32		0.39	
Mg	0.92	0.23	0.89	0.38	1.46	0.28		0.27	1.41
A1	0.93		0.32	0.24	2.06	2.12	0.56		0.53
Si	2.54	1.05	8.47	7.07	6.06	3.58	2.34	39.38	2.31
S	0.56	0.85	1.07	0.75	1.8	0.57	2.70	1.98	4.34
Cl	0.59	0.71	1.1	0.18	0.53	0.4	0.74	0.36	0.76
K	0.86	0.84	0.19		0.3	1.47	0.31	0.18	0.39
Ca	2.35	1.75	1.52	0.91	3.59	1.28	2.04	0.96	2.14
Ti			0.05	0.05					
V			0.13						
Cr	0.35	0.31	0.36	0.33				0.15	
Mn	0.65	0.58	0.58	0.53	0.48	0.6			
Fe	64.69	55.88	60.4	49.02	40.16	51.23	47.93	0.42	42.11
Co			0.21	0.52	0.31	0.42		0.06	
Zn	0.05		0.02		0.23		0.68		0.99
As	0.08		0.05	0.05	0.03				
Sn				0.64					
Sb	0.39		0.11	0.13	0.89	0.09	0.42		0.28
Ba			2.49	4.1	4.1	1.69	10.41	1.27	18.56
Total:	100.00	100.00	100.00	100.00	100.00	100.00	100.00	100.00	100.00
Mn/Fe	0.010	0.010	0.010	0.011	0.012	0.012	–	–	–

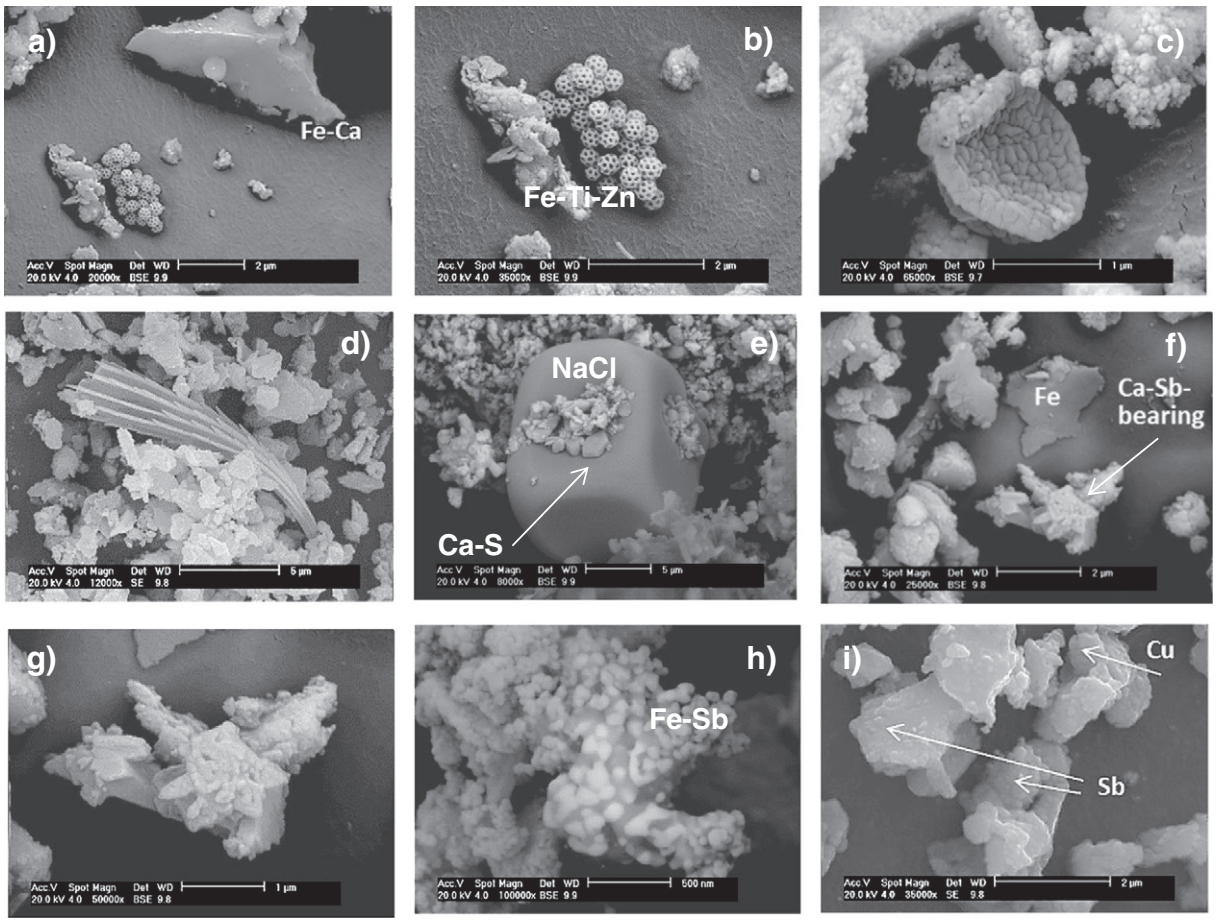

Fig. 3. SEM images of particles other than typical FePM also present in subway samples: a) Angular FePM splinter with attached calcium carbonate and (below left) cluster of nanometric spheres, brochosomes, secreted by leafhoppers; b) Close-up of brochosomes alongside nanometric cluster of metallic PM; c) Pollen grain; d) Insect fragment; e) Halite cube (with surface crystals of gypsum) growing on PUF substrate; f) FePM flakes alongside polycrystalline particle rich in Ca and Sb; g) Close up of CaSb particle; h) FePM rich in Sb and interpreted as derived from brake pad abrasion; i) Brake flakes containing Sb and Cu.

et al., 2012 and references therein). Carbonaceous particles in the subway environment, excluding those imported from above ground and those created by oxidation reactions of volatile organic compounds, can source from the high resistance commutator brushes in the electric motor and train pantographs connecting to the catenary. As discussed below, however, we consider that most of the subway-generated carbonaceous particles on station platforms are derived from interaction between the brake pad and train wheel. Train brakes in the Barcelona subway can be frontal or lateral dependent on the train model, and are chemically either carbonaceous-Fe poor (frontal pads: C> > Fe) or ferruginous–carbonaceous (lateral pads: Fe > C) (own data). As is the case with road traffic brake pads (Amato et al., 2012) the main chemical components of the train brake pads are heterogeneously distributed within the pad and accompanied by a wide spectrum of other cations such as Mg, Ca, Ba, Cr, Co, Sr, and Mo. Iron-poor pads (frontal types) additionally contain enhancements in a range of typical "crustal" elements (Al, Na, Ti, Li, V, Rb, Y, Nb, Th, U, and lanthanoid group, especially La, Ce, Pr and Nd) whereas metallic pads contain higher Mn, Ni, and especially Zn, Cu, As, Sb, and in some cases Pb (own data). Barium is a particularly characteristic component within the brakes utilised in the Barcelona metro, and in some pads can be abundant enough to comprise the dominant cation, combined with S in the form of barium sulphate (Table 1).

Examples of the distribution of trace elements within subway FePM are provided by the TEM data in Fig. 4 with images of low C FePM (C <2 wt.%, Fig. 4a) and medium C FePM (C <20 wt.%, Fig. 4b–d). The first example (Fig. 4a) shows a cluster of micrometric-sized angular MnCr steel fragments (centre and upper part of image) interpreted as produced by frictional processes at the wheel–rail interface. The particles appear relatively unoxidised and may therefore have been freshly generated just prior to collection. They are accompanied by Al-silicate and MgAl-silicate (lower and left part of image), and calcium carbonate (lower centre) particles. Fig. 4b offers a close-up of a single micrometric carbonaceous FePM in a more advanced state of oxidation. This particle contains traces of Si, Ca, Mn, and Co, and there is a markedly inhomogeneous distribution of Ba and S. The presence of these minor elements, especially Ba, along with the highly ferruginous nature of the particles, leads us to interpret this FePM as derived from a metallic lateral brake–wheel interface. Fig. 4c images two FePM flakes, both of which are again highly oxidised, carbonaceous, contain Si, Ca, and Al and are rich in barium and sulphur. These are also interpreted as metallic lateral brake particles and show a typically inhomogeneous distribution of zinc which is clustered into nuggets in the lower particle. Finally Fig. 4d provides a close-up of the lower brake flake imaged in Fig. 4c. At these magnifications the nugget-like texture displayed by Zn distribution is even more obvious, and it becomes increasingly clear that the secondary electron image of Fe itself has a mottled appearance implying internal inhomogeneity.

We zoom further into the detailed microstructure of these FePM flakes in Fig. 5, initially with an imaging sequence from Fig. 5a to c. The image in Fig. 5a may be compared to the featheredge of the flake shown in Fig. 4d (top of the image), and itself has ultrathin featheredges which again display the same mottled appearance. This texture becomes clearer in Fig. 5b and c, which reveals the mottling to comprise clusters of mostly rounded ferruginous nanocrystals typically

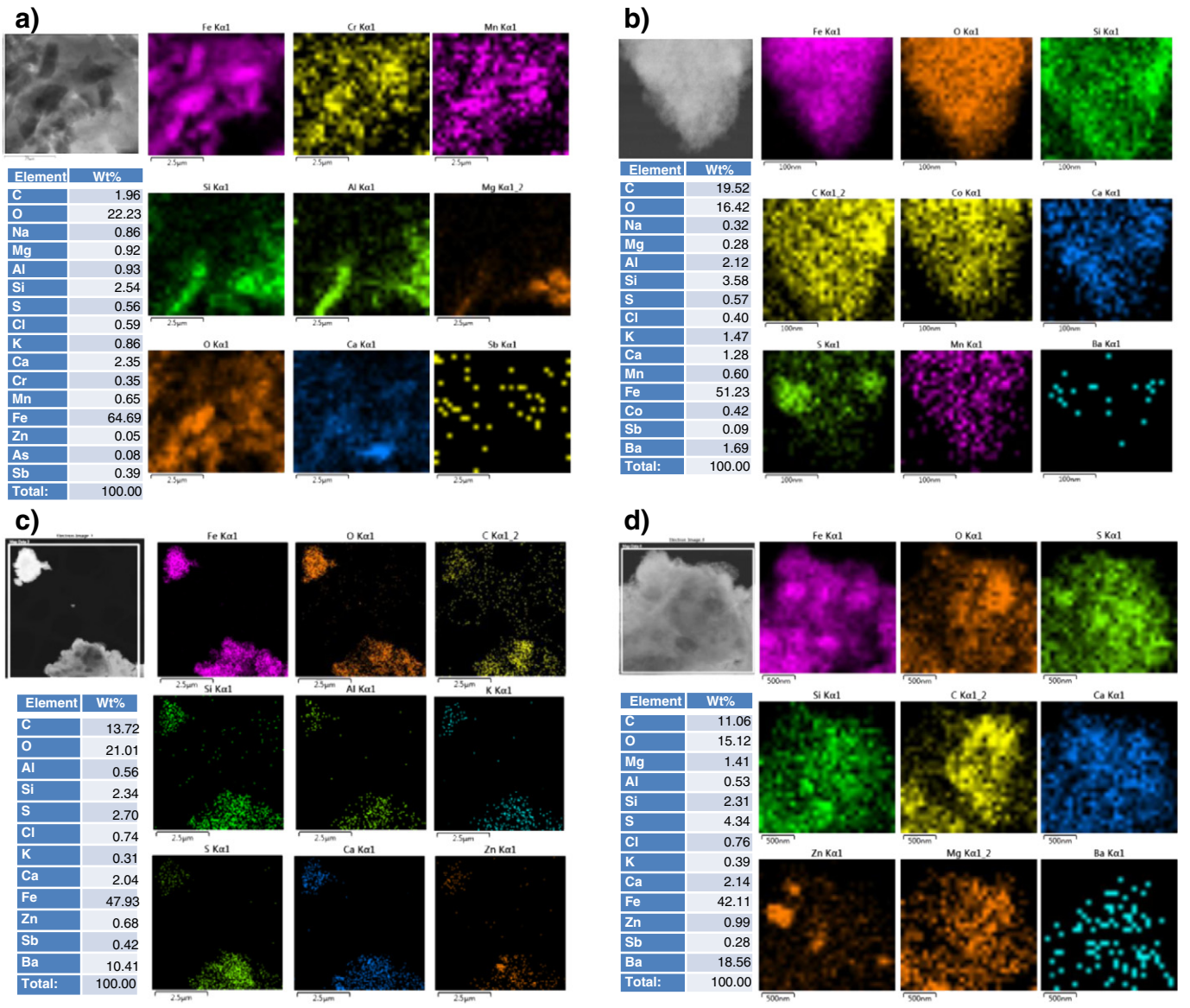

Fig. 4. TEM elemental mapping of Barcelona subway PM_{10} samples showing, a) Agglomerate of steel wheel/rail splinters and mineral dust particles; b) Oxidised steel FePM containing Si, C, Co, Ca, S, Mn and Ba, and interpreted as derived from metallic lateral brake pad: note inhomogeneous distribution of Ba and S; c–d) Brake flake particles showing inhomogeneous distribution of trace components and mottled nanocrystalline structure of iron oxide (continue to Fig. 5a–c).

measuring from 10 nm or less to a few 10s of nm. The highly crystalline nature of these samples is very apparent under the TEM, as demonstrated by an abundance of diffraction patterns available to determine the particle structure and lattice spacing. Thus most TEM images reveal the presence of nanocrystalline magnetite (Fig. 5d, e) and hematite (Fig. 5f), as well as onion-like concentric layers (Fig. 5g) indicative of carbon nanoparticle structure integrated within the FePM microstructure. The nanometric aggregates are not entirely iron oxide and carbon, however, as other tiny particles of compounds such as barium sulphate, barium carbonate, and halite can be identified (Fig. 5f, h).

Although the previous X-ray diffraction data from platform dust (Querol et al., 2012) have indicated that the bulk of Fe-particles in the Barcelona subway are present as hematite (Fe_2O_3), it is clear under the TEM that magnetite also exists within these nanometric aggregates, and in some places it is possible to identify the presence of Fe metal. One such FePM preserved native Fe is imaged in Fig. 5i as a slit-like core revealed inside a cracked submicron Fe particle with an oxidised coating. The stretching and cracking of this particle during submicron-scale oxidation are attributed to the stresses induced by a smaller lattice parameter of the oxidised shell as compared to the less oxidised core (Feitknecht and Gallagher, 1970; Özdemir et al., 1993). The enduring presence of iron metal within platform FePM, however, is the exception: most inhalable-sized platform FePM flakes are composed of iron oxide nanocrystals within which are intimately incorporated nanocrystals of other compounds originally also present within the parent materials.

4. Discussion

Our observations on subway platform particles confirm that they are pervasively ferruginous and both physically and chemically different from the typical outdoor urban cocktail of inhalable PM breathed above ground in the city. This in turn indicates that the dominant mix of source materials and processes of PM generation are unique to the subway environment. This conclusion is nothing new: a considerable number of papers published on subway PM over the last ten years

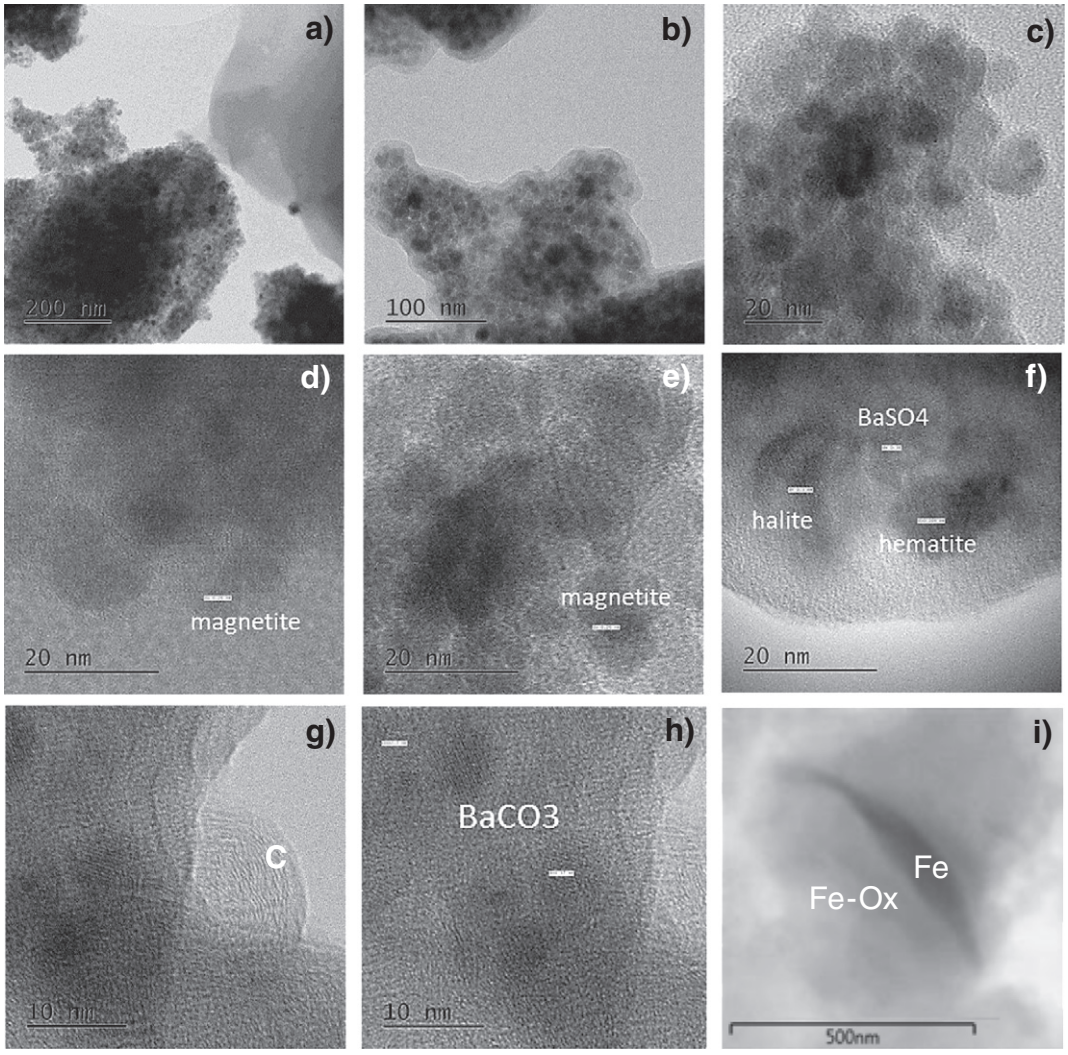

Fig. 5. High magnification images of FePM composed of iron oxide nanocrystals (a–c) containing magnetite (d, e), hematite (f), concentric carbon nanocrystals (g), barium salts (f, h) and halite (f). Fig. 5i images a cracked nanoparticle revealing an iron metal core and oxidised shell: see text for discussion.

have highlighted the ferruginous nature of such aerosols and concluded that the obvious sources distinctive to the subway are related to train movement, with wheels, rails, brakes, and electrical supply system all implicated in FePM generation. However, reading the available literature can reveal a lack of precision over the relative importance of these different sources, the specific processes that generate different FePM, and whether subway aerosols are more toxic than those breathed at street level. In this context, the following discussion section will focus on FePM chemical composition, oxidation history, microstructure, generation processes, and conclude with a brief comment on concerns over potential toxicity.

Our current understanding of the chemical speciation of subway FePM owes much to a series of publications on air quality in the Seoul underground rail system of South Korea (e.g. Kang et al., 2008; Kim et al., 2010; HJ. Jung et al., 2012; Eom et al., 2013). Ambient $FePM_{10}$ in the tunnel and platform has been recorded as comprising a mixture of iron metal (α-Fe), magnetite (Fe_3O_4), maghemite (γ-Fe_2O_3) and hematite (α-Fe_2O_3), with unoxidised Fe-metal being less common than oxide, and a majority of FePM being carbonaceous. Samples of subway dusts appear to be more magnetic if collected closer to the rail, indicating the presence of more iron metal, magnetite and maghemite relative to non-magnetic hematite (HJ. Jung et al., 2012), and revealing spatial variation in the oxidation state of FePM. Similarly, in those stations with platform sliding doors, ambient FePM has been reported to be less ferruginous and less magnetic (Kim et al., 2010; HJ. Jung et al., 2012), this presumably reflecting reduced amounts of fresh tunnel-generated Fe-metal-bearing particles gaining access to the platform.

One of the commonest oxide mineral reactions in nature is the oxidation of magnetite to maghemite (Özdemir et al., 1993), which is in turn metastable relative to hematite (Guo and Barnard, 2013; Machala et al., 2011). The presence of a mixture of iron metal and various oxides in the same subway particle, with the oxides sometimes seen as an external carapace (e.g. Fig. 5i), presumably records stages in the progressive oxidation of freshly exposed highly active metal surfaces of iron splinters and flakes to magnetite, maghemite and hematite, with smaller particles having greater surface areas available for reaction (Kang et al., 2008; Knibbs et al., 2011; HJ. Jung et al., 2012; Eom et al., 2013). One of the key, and perhaps surprising, characteristics of inhalable subway particles is that most of them are extremely small, as shown in our study and as emphasised in several other recent publications (e.g. Jansson et al., 2010; HJ. Jung et al., 2012; Midander et al., 2012; Loxham et al., 2013). Indeed there appears to be an increasing realisation that ferruginous nanoparticulate material (nanoFePM) is the dominant inhalable aerosol in the subway environment and that it is not necessary to invoke the traditional view that such materials are produced by high temperature processes such as vapourisation and

condensation. This new understanding stems from the combination of direct observation of subway PM (as in our study) with the results from experimental studies (e.g. Olofsson, 2011; Sundh et al., 2009; Abbasi et al., 2012). Wear rates and particle generation at the train rail–wheel contact can be shown both to increase with increasing load and produce a large amount of ultrafine PM in the size range 0.25–1 μm (Sundh et al., 2009). Similarly, disc brake PM released from regional trains contains abundant amounts of nanometric particles which can be as small as 50 nm (Abbasi et al., 2012). In a particularly revealing study, Olofsson (2011) produced frictionally-generated nanoparticles by simulating the sliding of brake materials against railway wheels, and demonstrated that under their chosen experimental conditions metalliferous brake pads generate many more nanoFePM than composite pads.

Much of the finer inhalable FePM on subway platforms in the Barcelona metro comprises iron oxide nanocrystal aggregates like those imaged in Fig. 5. These nanoFePM have been observed by some of the few previous subway publications to utilise TEM, with Salma (2009) describing structured aggregates of rounded crystals 5–15 nm in size, and Zhang et al. (2011) recording "clumped" submicron-sized magnetic FePM. These nanoFePM materials are commonly flake-like in form which, rather than suggesting condensation of Fe vapour (Kang et al., 2008; Salma, 2009; Salma et al., 2009; HJ. Jung et al., 2012; Loxham et al., 2013) we interpret as generated mechanically by frictional wear, especially by the sliding of two metallic surfaces such as between lateral brake pads and wheel, followed by oxidation. Their parent material is steel or cast iron which has become pervasively, but not always completely, oxidised to magnetic oxide species (magnetite and maghemite) and non-magnetic hematite. The morphologies of natural magnetite nanoparticles are octahedral and rhombo-dodecahedral (Guo and Barnard, 2013), a microtexture preserved even when further oxidation produces maghemite as this mineral simply pseudomorphs the pre-existing magnetite without creating a new crystal form. Suggestions of formerly euhedral nanocrystals with octahedral form are discernable in some of the ferruginous flakes (e.g. Fig. 5c). However, further conversion to hematite alters the magnetic microstructure texture to produce more rounded crystal forms. We invoke the partial or total replacement of precursor magnetic minerals by non-magnetic hematite to explain the typically less well-defined crystal faces in more amorphous aggregates such as those depicted in our subway PM images (Fig. 5). Our images of nanometric FePM magnetite–maghemite clusters are similar to those of naturally occurring iron magnetite–maghemite–hematite nanocrystals (Guo and Barnard, 2013).

Our chemical data on individual platform FePM indicates that many of them are brake flakes, namely slices of oxidised ferruginous and carbonaceous material dissociated from the brake pad (Fig. 4b, c) during brake application immediately prior to and during station entry. Brake dust is not, of course, exclusive to subway air, being abundantly generated by road traffic in outdoor city air, although diluted by the products of hydrocarbon combustion and particle resuspension. Sagnotti et al. (2009) for example identified outdoor brake flakes forming rough-surfaced particles of non-stoichiometric nanocrystalline magnetite with an inhomogeneous microchemistry and a morphology "remarkably different from the typical spherical particles of industrial fly ashes". In the case of the rail subway, brake flakes will be swept through and settle in the station under the diminishing influence of each train arrival piston effect. These subway brake flakes, undiluted by road vehicle emissions, are therefore expected to be much more common on the platform than in the tunnel or outdoors. In addition to the brake flakes, many other platform FePM will be derived from the chemically more homogeneous Mn steel of the wheel and/or rails, as demonstrated by their distinctive trace element chemistry (such as a Mn/Fe ratio of 0.01: Fig. 4a, b). Although we have emphasised the overwhelmingly dominant role of mechanical processes in the generation of the Barcelona metro atmospheric environment, where few particles are spheroidal, this will not be necessarily the case for all other systems worldwide. In the Seoul subway, for example, the descriptions of Eom et al. (2013) indicate the more obvious presence of micrometric Fe-spheres which they attribute to iron metal sparking vapourisation followed by condensation, analogous to particle generation during arc-welding. Also the passing of diesel trains during nightwork can help the formation of particles by condensation and thermal fragmentation of nanoparticle aggregates (Burchill et al., 2011).

Finally, we return to the subject of FePM toxicity and the possibility that subway air is more capable of damaging human health than city air outdoors. The main evidence in favour of subway FePM being more genotoxic and capable of inducing oxidative stress has been presented by Karlsson et al. (2005) using platform PM_{10} collected on glass fibre filters (see also Karlsson et al., 2006, when part of the subway sample bioreactivity was found to be due to the lingering presence of glass filter fibres in the extracted samples). They considered their FePM samples to be mostly magnetite, although in a subsequent study (Karlsson et al., 2008) they were unable to prove their original speculation that high Fe content was behind an increased ability to induce oxidative stress. Comparisons with various samples of magnetite, hematite, Cu and Cu–Zn failed to produce the same toxic response (Karlsson et al., 2008). Papers subsequently published on rail-generated particles usually quote at least one of these papers (e.g. Kang et al., 2008; Salma, 2009; Murruni et al., 2009; Olofsson, 2011; Zhang et al., 2011; Múgica-Alvarez et al., 2012; HJ. Jung et al., 2012; Midander et al., 2012; Abbasi et al., 2013; Eom et al., 2013; Loxham et al., 2013; Querol et al., 2012; Moreno et al., 2014). In a study of PM subway doses Seaton et al. (2005) reached the conclusion that "those principally at risk from dust inhalation by working or travelling in the London Underground should not be seriously concerned, although efforts to reduce dust concentrations should continue, since the dust is not without toxicity". With regard to epidemiological evidence, Gustavsson et al. (2008) concluded that no increased lung cancer risk was found amongst subway train drivers, and their study thus failed to support any hypothesis that subway particles are more potent in inducing lung cancer than particles in ambient air. Given the uncertain and limited nature of the evidence for subway metalliferous PM toxicity, there appears to us to be no obvious cause for alarmist concern, although given the peculiar metal chemistry of these particles, with enhanced amounts of toxic trace elements such as Mn and Cr (e.g. see Chillrud et al., 2004), the presence of nanocrystals of magnetite and maghemite (Park et al., 2014), and the possibility that some brake pad materials may produce more toxic flakes than others, adoption of the precautionary principle would seem wise. Thus, as with outside city air in traffic hot spots (where toxicological effects have been demonstrated, Janssen et al., 2012; Sysalová et al., 2012), at this stage the priority in subway air quality should be to reduce the high mass concentrations of aerosol present in some stations rather than worry about attempting to remove some chemical component of unspecified toxicity.

5. Conclusions

1. Ambient subway platform aerosol particles mostly source from train movement and are pervasively ferruginous (FePM), commonly carbonaceous, and both physically and chemically distinctive from PM breathed in outdoor urban air.
2. The most common form of subway FePM is very small (nanometric up to a few microns in size) and derives dominantly from mechanical processes of sliding and wear at the brake–wheel and wheel–rail interfaces, with, in Barcelona at least, only minor contributions from high temperature processes such as sparking.
3. Metallic flakes and splinters released from the wheel area undergo progressive atmospheric oxidation from native iron through magnetite, maghemite and hematite organised within a nanocrystalline oxide matrix which images as a distinctive mottled nanostructure under TEM. Individual nanocrystals, now mostly hematite, are typically 10–20 nm and rounded in appearance, although they can

preserve remnants of octahedral forms indicative of their origin as magnetite derived from the oxidation of iron metal.

4. The chemistry of individual FePM under TEM allows differentiation between different anthropogenic sources, such as an origin from Mn steel (wheels, rail) or brake pads. Particles released during frictional brake wear in particular exhibit a highly distinctive "brake flake" chemistry marked by the inhomogeneous distribution of unusual trace elements such as barium, and their incorporation into the ferruginous nanocrystalline structure.
5. It is still unclear whether subway is more or less toxic than outdoor air. Hematite, one of the toxicologically more benign iron oxides, is the dominant FePM species on station platforms so that any subway air health effects may relate more to high inhalable mass levels than their metallic chemistry.

Acknowledgments

This work was supported by the Spanish Ministry of Economy and Competitiveness and FEDER funds within the I + D Project CGL2012-33066 (METRO), the European Union Seventh Framework Programme (FP7/2007–2013) under grant agreement no. 315760 HEXACOMM and the IMPROVE LIFE project (LIFE13 ENV/ES/000263). F. Amato is beneficiary of an AXA Research Fund postdoctoral grant. We acknowledge useful discussion with our colleague Greg Power.

References

Aarnio P, Yli-Tuomi T, Kousa A, Makela T, Hirsikko A, Hammeri K, et al. The concentrations and composition of and exposure to fine particles (PM2.5) in the Helsinki subway system. Atmos Environ 2005;39(28):5059–66.

Abbasi S, Jansson A, Olander L, Olofsson U, Larsson C, Sellgren U. A field test study of airborne wear particles from a running regional train. Int J Rail Rapid Transit 2012;226(1):95–109.

Abbasi S, Jansson A, Sellgren U, Olofsson U. Particle emissions from rail traffic: a literature review. Crit Rev Environ Sci Technol 2013;43:2511–44.

Amato F, Font O, Moreno N, Alastuey A, Querol X. Mineralogy and elemental composition of brake pads of common use in Spain. Macla 2012;16:154–6.

Braniš M. The contribution of ambient sources to particulate pollution in spaces and trains of the Prague underground transport system. Atmos Environ 2006;40:348–56.

Burchill M, Gramotnev D, Gramotnev G, Davison B, Flegg M. Monitoring and analysis of combustion aerosol emissions from fast moving diesel trains. Sci Total Environ 2011;409:985–93.

Cheng YH, Yan JW. Comparisons of PM, CO, and CO_2 levels in underground and ground-level stations in the Taipei mass rapid transit system. Atmos Environ 2011;45:4882–91.

Chillrud SN, Epstein D, Ross JM, Sax SN, Pederson D, Spengler JD, et al. Elevated airborne exposures of teenagers to manganese, chromium, and steel dust and New York City's subway system. Environ Sci Technol 2004;38:732–7.

Colombi C, Angius S, Gianelle V, Lazzarini M. Particulate matter concentrations, physical characteristics and elemental composition in the Milan underground transport system. Atmos Environ 2013;70:166–78.

Eom HY, Jung HJ, Sobanska S, Chung SG, Son YS, Kim JC, et al. Iron speciation of airborne subway particles by the combined use of energy dispersive electron probe X ray microanalysis and Raman microspectrometry. Anal Chem 2013;85:10424–31.

Feitknecht W, Gallagher KJ. Mechanisms for the oxidation of Fe_3O_4. Nature 1970;228(5271):548–9.

Fromme H, Oddoy A, Piloty M, Krause M, Lahrz T. Polycyclic aromatic hydrocarbons (PAH) and diesel Engine emission (EC) inside a car and a subway train. Sci Total Environ 1998;217:165–73.

Guo H, Barnard A. Naturally occurring iron oxide nanoparticles: morphology, surface chemistry and environmental stability. J Mater Chem A 2013;1:27–42.

Gustavsson P, Bigert C, Pollan M. Incidence of lung cancer among subway drivers in Stockholm. Am J Ind Med 2008;51:545–7.

Janssen N, Gerlofs-Nijland M, Lanki T, Salonen R, Cassee F, Hoek G, et al. Health effects of black carbon. WHO; 2012 (ISBN: 978 92 890 0265 3. http://www.euro.who.int/__data/assets/pdf_file/0004/162535/e96541.pdf).

Jansson A, Olander L, Olofsson U, Sundh J, Söderberg A, Wahlström J. Ultrafine particle formation from wear. Int J Vent 2010;9:83–8.

Johansson C, Johansson PA. Particulate matter in the underground of Stockholm. Atmos Environ 2003;37:3–9.

Jung M, Kim H, Park Y, Park D, Chung K, Oh S. Genotoxic effects and oxidative stress induced by organic extracts of particulate matter (PM10) collected from a subway tunnel in Seoul, Korea. Genet Toxicol Environ Mutagen 2012;749:39–47.

Jung HJ, Kim B, Malek M, Koo Y, Jung J, Son YS, et al. Chemical speciation of size-segregated floor dusts and airborne magnetic particles collected at underground subway stations in Seoul, Korea. J Hazard Mater 2012;213-214:331–40.

Kam W, Cheung K, Daher N, Sioutas C. Particulate matter concentrations in underground and ground-level rail systems of the Los Angeles Metro. Atmos Environ 2011;45:1506–16.

Kang S, Hwang H, Park Y, Kim H, Ro CU. Chemical compositions of subway particles in Seoul, Korea determined by a quantitative single particle analysis. Environ Sci Technol 2008;42:9051–7.

Karlsson HL, Nilsson L, Möller L. Subway particles are more genotoxic than street particles and induce oxidative stress in cultured human lung cells. Chem Res Toxicol 2005;18:19–23.

Karlsson H, Ljungman A, Lindbom J, Möller L. Comparison of genotoxic and inflammatory effects of particles generated by wood combustion, a road simulator and collected from street and subway. Toxicol Lett 2006;165:203–11.

Karlsson HL, Holgersson A, Möller L. Mechanisms related to the genotoxicity of particles in the subway and from other sources. Chem Res Toxicol 2008;21:726–31.

Kim KY, Kim YS, Roh YM, Lee CM, Kim CN. Spatial distribution of PM10 and PM2.5 in Seoul Metropolitan Subway stations. J Hazard Mater 2008;154:440–3.

Kim Y, Kim M, Lim J, Kim JT, Yoo C. Predictive monitoring and diagnosis of periodic air pollution in a subway station. J Hazard Mater 2010;183(1–3):448–59.

Knibbs L, Cole-Hunter T, Morawska L. A review of commuter exposure to ultrafine particles and its health effects. Atmos Environ 2011;45:2611–22.

Loxham M, Cooper MJ, Gerlofs-Nijland ME, Cassee F, Davies DE, Palmer MR, et al. Physicochemical characterization of airborne particulate matter at a mainline underground railway station. Environ Sci Technol 2013;47:3614–22.

Machala L, Tucek J, Zboril R. Polymorphous transformations of nanometric iron(III) oxide: a review. Chem Mater 2011;23:3255–72.

Midander K, Elihn K, Wallén A, Belova L, Borg Karlsson A, Wallinder I. Characterisation of nano- and micron-sized airborne and collected subway particles, a multi-analytical approach. Sci Total Environ 2012;427-428:390–400.

Minguillón MC, Schembari A, Triguero-Mas M, de Nazelle A, Dadvand P, Figueras F, et al. Source apportionment of indoor, outdoor and personal PM2.5 exposure of pregnant women in Barcelona, Spain. Atmos Environ 2012;59:426–36.

Moreno T, Pérez N, Reche C, Martins V, de Miguel E, Capdevila M, et al. Subway platform air quality: assessing the influences of tunnel ventilation, train piston effect and station design. Atmos Environ 2014;92:461–8.

Múgica-Alvarez V, Figueroa-Lara J, Romero-Romo M, Sepúlveda-Sánchez J, López-Moreno T. Concentrations and properties of airborne particles in the Mexico City subway system. Atmos Environ 2012;49:284–93.

Murruni L, Solanes V, Debray M, Kreiner A, Davidson J, Davidson M, et al. Concentrations and elemental composition of particulate matter in the Buenos Aires underground system. Atmos Environ 2009;43:4577–83.

Nieuwenhuijsen MJ, Gómez-Perales E, Colvile RN. Levels of particulate air pollution, its elemental composition, determinants and health effects in metro systems. Atmos Environ 2007;41:7995–8006.

Olofsson U. A study of airborne wear particles generated from the train traffic — block braking simulation in a pin-on-disc machine. Wear 2011;271:86–91.

Özdemir Ö, Dunlop D, Moskowitz B. The effect of oxidation on the Verwey transition in magnetite. Geophys Res Lett 1993;20:1671–4.

Park D, Ha K. Characteristics of PM10, PM2.5, CO_2 and CO monitored in interiors and platform of subway train in Seoul, Korea. Environ Int 2008;34:629–34.

Park E, Umh H, Choi D, Cho M, Choi W, Kim S, et al. Magnetite and maghemite induced different toxicity in murine alveolar macrophage cells. Arch Toxicol 2014. http://dx.doi.org/10.1007/s00204-014-1210-1.

Querol X, Moreno T, Karanasiou A, Reche C, Alastuey A, Viana M, et al. Variability of levels and composition of PM10 and PM2.5 in the Barcelona metro system. Atmos Chem Phys 2012;12:5055–76.

Raut JC, Chazette P, Fortain A. Link between aerosol optical, microphysical and chemical measurements in an underground railway station in Paris. Atmos Environ 2009;43:860–8.

Ripanucci G, Grana M, Vicentini L, Magrini A, Bergamaschi A. Dust in the underground railway tunnels of an Italian town. J Occup Environ Hyg 2006;3:16–25.

Sagnotti L, Taddeucci J, Winkler A, Cavallo A. Compositional, morphological, and hysteresis characterization of magnetic airborne particulate matter in Rome, Italy. Geochem Geophys Geosyst 2009;10. http://dx.doi.org/10.1029/2009GC002563.

Salma I. Issues in environmental science and technology. In: Hester RE, Harrison RM, editors. Royal Society of Chemistry; 2009. (28).

Salma I, Weidinger T, Maenhaut W. Time-resolved mass concentration, composition and sources of aerosol particles in a metropolitan underground railway station. Atmos Environ 2007;41:8391–405.

Salma I, Posfai M, Kovacs K, Kuzmann E, Homonnay Z, Posta J. Properties and sources of individual particles and some chemical species in the aerosol of a metropolitan underground railway station. Atmos Environ 2009;43:3460–6.

Seaton A, Cherrie J, Dennekamp M, Donalson K, Hurley F, Tran L. The London underground: dust and hazards to health. Occup Environ Med 2005;62:355–62.

Sundh J, Olofsson U, Olander L, Jansson A. Wear rate testing in relation to airborne particles generated in a wheel–rail contact. Lubr Sci 2009;21:135–50.

Sysalová J, Sýkorová I, Havelcová M, Száková J, Trejtnarová H, Kotlík B. Toxicologically important trace elements and organic compounds investigated in size-fractionated urban particulate matter collected near the Prague highway. Sci Total Environ 2012;437:127–36.

Ye X, Lian Z, Jiang Ch, Zhou Z, Chen H. Investigation of indoor environmental quality in Shanghai metro stations, China. Environ Monit Assess 2010;167:643–51.

Zhang W, Jiang H, Dong C, Yan Q, Yu L, Yu Y. Magnetic and geochemical characterization of iron pollution in subway dusts in Shanghai, China. Geochem Geophys Geosyst 2011;12:Q06Z25. http://dx.doi.org/10.1029/2011GC003524.